Electron Diffraction with the Amorphous Alloys $Fe_{80}B_{20}$ and $Mn_{73}Si_{27}$

F. Paasche, H. Olbrich, G. Rainer-Harbach, P. Lamparter, and S. Steeb
Max-Planck-Institut für Metallforschung, Institut für Werkstoffwissenschaften, Stuttgart

Z. Naturforsch. **37 a**, 1215–1222 (1982); received July 8, 1982

Electron diffraction with amorphous $Fe_{80}B_{20}$ and $Mn_{73}Si_{27}$ yields structure factors and pair correlation functions which are discussed together with the results of X-ray- and neutron-diffraction experiments. For $Mn_{73}Si_{27}$ additional interesting details are revealed. A tetrahedral model for $Mn_{73}Si_{27}$ is described. Finally we show that the evaluation of partial structure factors by the three beam experiment, i.e. the combination of an electron-, X-ray- and neutron-diffraction experiment is not possible in general.

Introduction

Recently the partial structure factors of amorphous $Fe_{80}B_{20}$ [1], and under restrictions also of $Mn_{73}Si_{27}$ [2], have been determined by means of X-ray- and neutron-diffraction. Since a newly developed SHEED-apparatus [3] is now available, in this paper these substances have been investigated by electron diffraction. The obtained total structure factors are discussed together with the results obtained in [1, 2]. A method for the correction for the influence of multiple scattering given in [3] has been used in the quantitative evaluation of the electron diffraction patterns.

Theoretical Fundamentals

For a binary alloy the three partial distribution functions g_{AA}, g_{BB}, and g_{AB} contribute to the total pair distribution function:

$$g(r) = \frac{c_A^2 f_A^2}{\langle f^2\rangle} g_{AA}(r) + \frac{c_B^2 f_B^2}{\langle f^2\rangle} g_{BB}(r) + \frac{2 c_A c_B f_A f_B}{\langle f^2\rangle} g_{AB}(r) \quad (1)$$

with $c_{A,B}$ = atomic fraction of component A, B, $f_{A,B}$ = scattering length of component A, B, and $\langle f^2\rangle = c_A f_A^2 + c_B f_B^2$.

The three partial structure factors $S_{AA}(Q)$, $S_{BB}(Q)$, and $S_{AB}(Q)$ contribute to the total structure factor $S(Q)$:

$$S(Q) = \frac{c_A f_A^2}{\langle f^2\rangle} S_{AA}(Q) + \frac{c_B f_B^2}{\langle f^2\rangle} S_{BB}(Q) + \frac{2\sqrt{c_A c_B} f_A f_B}{\langle f^2\rangle} S_{AB}(Q) \quad (2)$$

with $Q = 4\pi \sin\theta/\lambda$ and λ = wavelength of the radiation used.

The total structure factor is obtained from the coherently scattered intensity $I(Q)$:

$$S(Q) = \frac{I_{koh}(Q)}{N\langle f^2(Q)\rangle} \quad (3)$$

with N = normalization constant.

The connection between $g(r)$ and $S(Q)$ is given by

$$4\pi\varrho_0 r\left[g(r) - \frac{\langle f\rangle^2}{\langle f^2\rangle}\right] = \frac{2}{\pi}\int_0^\infty Q[S(Q) - 1]\sin(Qr)\,dQ \quad (4)$$

with $\langle f\rangle = c_A f_A + c_B f_B$.

The pair correlation function $G(r)$ describes the deviation of the local number density $\varrho(r)$ from the mean number density ϱ_0:

$$G(r) = 4\pi r\left[\varrho(r) - \frac{\langle f\rangle^2}{\langle f^2\rangle}\varrho_0\right] = 4\pi\varrho_0 r\left[g(r) - \frac{\langle f\rangle^2}{\langle f^2\rangle}\right]. \quad (5)$$

Integration of the radial distribution function

$$A(r) = 4\pi r^2\cdot\varrho(r) = 4\pi r^2\frac{\langle f\rangle^2}{\langle f^2\rangle}\varrho_0 + r\cdot G(r) \quad (6)$$

Reprint requests to Prof. Dr. S. Steeb, Max-Planck-Institut f. Metallforschung, Institut f. Werkstoffwissenschaften, Seestraße 92, D-7000 Stuttgart 1.

0340-4811 / 82 / 1100-1215 $ 01.30/0. — Please order a reprint rather than making your own copy.

over the first maximum yields the corresponding coordination number.

The structure in a binary alloy can also be described using the correlation functions of the density- and concentration-fluctuations [4], i.e. by g_{NN} and g_{CC}. The mutual dependence of these two functions is described by the cross term g_{NC} and we obtain in analogy to (1)

$$g(r) = \frac{\langle f\rangle^2}{\langle f^2\rangle} g_{NN}(r) + \frac{c_A c_B (\Delta f)^2}{\langle f^2\rangle} g_{CC}(r) + \frac{2\langle f\rangle \Delta f}{\langle f^2\rangle} g_{NC}(r) \quad (7)$$

with

$$\Delta f = f_A - f_B .$$

The structure factor $S(Q)$ from (3) can be described in terms of the partial Bhatia Thornton structure factors which are the Fourier transforms of the corresponding correlation functions of (7):

$$S(Q) = \frac{\langle f\rangle^2}{\langle f^2\rangle} S_{NN}(Q) + \frac{c_A c_B (\Delta f)^2}{\langle f^2\rangle} S_{CC}(Q) + \frac{2\langle f\rangle \Delta f}{\langle f^2\rangle} S_{NC}(Q) . \quad (8)$$

g_{NN} describes the spatial correlation between density fluctuations, i.e. the deviation of the local density from the mean density. By g_{NN} the global structure of the system is described without distinction of the two kinds of atoms. g_{CC} describes the spatial correlation of concentration fluctuations. It contains information about the chemical short range order within the corresponding substance. For the statistical distribution of both kinds of atoms one obtains $g_{CC} = 0$. Distances between atoms of equal kind are represented by maxima of the function g_{CC}, distances between atoms of unequal kind by minima. Different size of the atoms causes the concentration- and density-fluctuations to depend from each other. This cross correlation is described by g_{NC}, which becomes zero for atoms of equal size.

Experiments, Evaluation, and Discussion

The preparation of the specimens was described in [5]. By melt spinning using a copper cylinder, amorphous ribbons with a thickness of 5 to 10 μm were produced. Thereby the rotation velocity of the cylinder was chosen as large as to obtain ribbons with a large amount of holes which on their circumference show areas convenient for the production of electron diffraction diagrams.

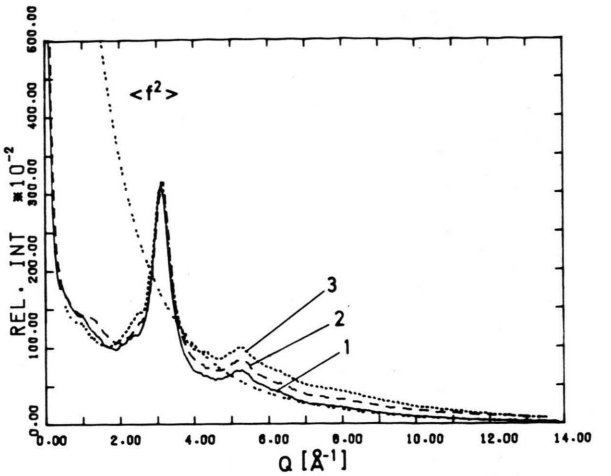

Fig. 1. Amorphous $Fe_{80}B_{20}$: Electron diffraction (50 kV): ——— run 1; ----- run 2; ..... run 3.

i) *$Fe_{80}B_{20}$*

Figure 1 shows three of the diffraction patterns obtained with amorphous $Fe_{80}B_{20}$, and the $\langle f^2\rangle$-curve. Using these curves, first of all the influence of *multiple scattering* shall be discussed. The solid line 1 shows good agreement with $\langle f^2\rangle$ for large Q's. The lines corresponding to runs 2 and 3 show an intensity distribution which is clearly influenced by multiple scattering (see [3]).

The evaluation showed that the accordance of the uncorrected curve with $N\langle f^2\rangle$ (Fig. 1), where N is the normalization constant, is no sufficient criterion for the necessity or unnecessity of a correction for multiple scattering. However, such a criterion exists if one wants to calculate the total structure factor according to (3). For example, curve 1 in Fig. 1 yields the solid line structure factor in Fig. 2 which does not oscillate around unity at higher Q-values. The behaviour in this region forms a good criterion for the choice of the parameter I/I_0 of the correction procedure for multiple scattering. The dashed line in Fig. 2 shows the total structure factor obtained using the optimized parameter I/I_0. Compared to the original curve, the corrected structure factor oscillates around unity up to very large Q's and is enhanced in the region of the first maximum. Though it is to be expected that by applying the correction procedure the split of the second maxi-

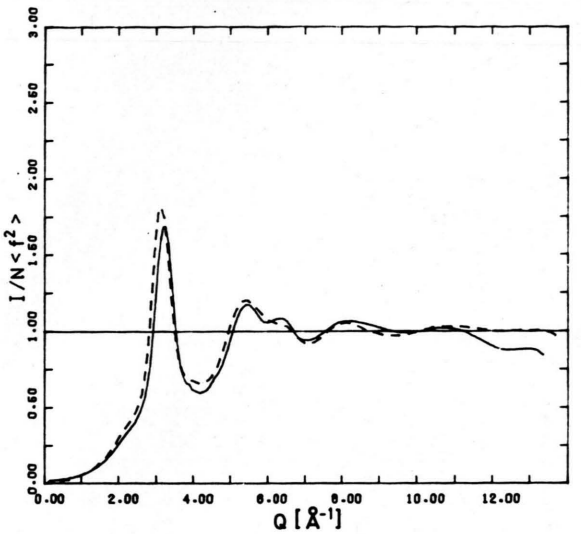

Fig. 2. Amorphous $Fe_{80}B_{20}$ (run 1): Electron diffraction (50 kV). $I/N\langle f^2\rangle$ versus Q: ——— without correction for multiple scattering; ----- with correction for multiple scattering (parameter $I/I_0 = 0.7$).

mum should become more pronounced we can state that in this region a loss of information caused by the correction procedure can be observed.

Figure 3 b shows the corrected experimental curve for the second run in Fig. 1 together with $N\langle f^2\rangle$. Compared to the uncorrected curve in Fig. 3 a the accordance with $N\langle f^2\rangle$ at higher Q's is improved and the maxima at lower Q's are enhanced. Using the criterion that for large Q the structure factor must become unity, the parameter I/I_0 for the multiple scattering correction could be determined with an uncertainty of ± 0.02. Thus the structure factor itself in the region of the main maximum contains an uncertainty of ± 0.2. In Fig. 4 the influence of I/I_0 on the structure factor is demonstrated. In Fig. 4 a the correction was too small whereas in Fig. 4 b it was too large.

To calculate the structure factor from the uncorrected curve one only needs the normalization and especially for thicker specimens the correction for multiple scattering. An absorption correction

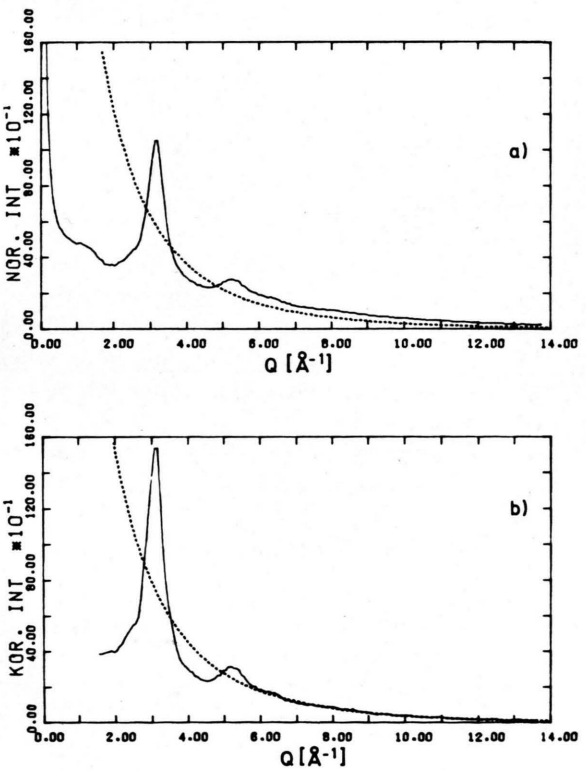

Fig. 3. Amorphous $Fe_{80}B_{20}$ (run 2): Electron diffraction (50 kV). Intensity versus Q: a) without correction for multiple scattering; b) with correction for multiple scattering (parameter $I/I_0 = 0.38$).

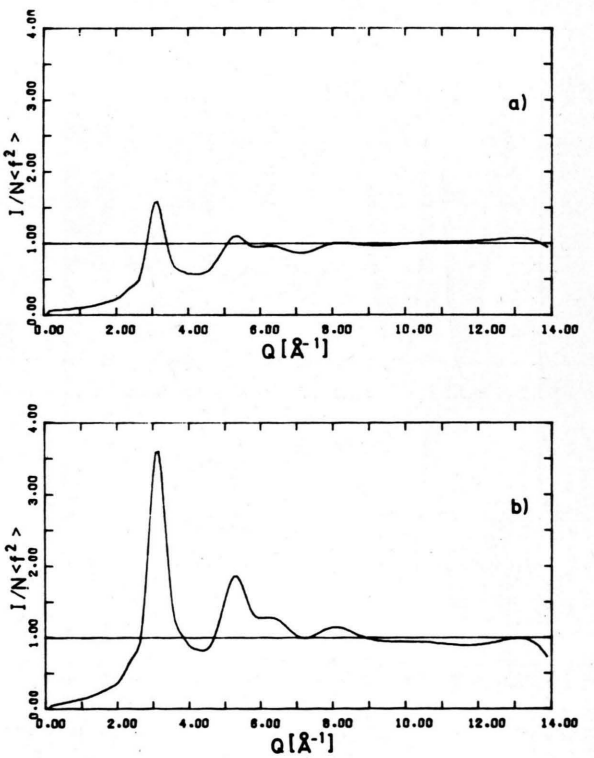

Fig. 4. Amorphous $Fe_{80}B_{20}$ (run 2): Electron diffraction (50 kV). $I/N\langle f\rangle$ versus Q: a) parameter $I/I_0 = 0.5$; b) parameter $I/I_0 = 0.2$.

can be neglected. The normalization procedure was done according to Krogh-Moe [6].

The results thus obtained with the three electron-Fe-B-experiments and the X-ray-Fe-B-experiment are given in Figure 5. The comparison with the corresponding X-ray structure factor according to [1] shows that the first maximum of the X-ray curve is larger by a factor of two, that the minimum between the first and second maxima of the X-ray diffraction curve is much more pronounced, and that the partial maximum at $Q = 6.5$ Å^{-1} is lower in the X-ray curve than in the electron curve. Furthermore the X-ray curve is less damped. It should be stressed that most of these differences could also be observed for amorphous Germanium (see [3]). In [3] these discrepancies, which are not

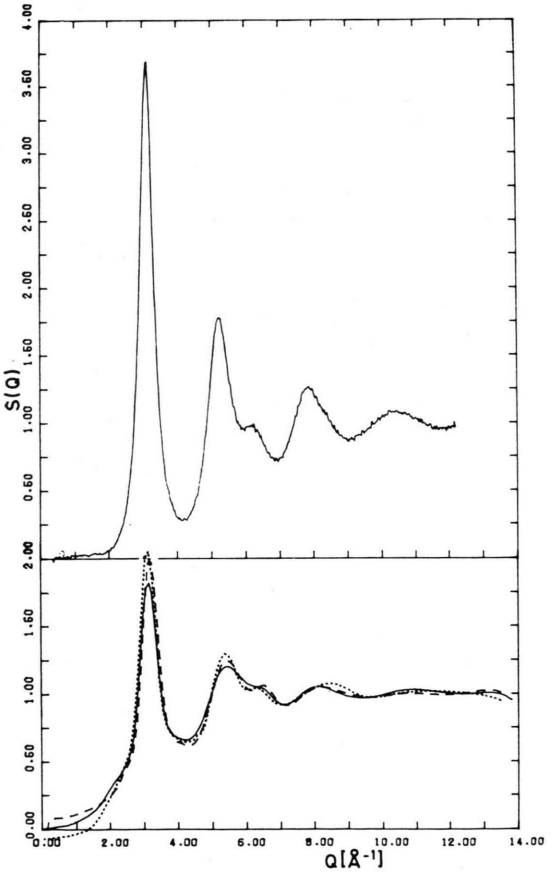

Fig. 5. Amorphous $Fe_{80}B_{20}$: Lower curves: Electron diffraction (50 kV). Structure factors: ——— run 1, $I/I_0 = 0.7$; ----- run 2, $I/I_0 = 0.38$; ..... run 3, $I/I_0 = 0.16$. Upper curve: X-ray-diffraction. Structure factor according to Ref. [1] but given in terms of the Ashcroft-Lekner definition.

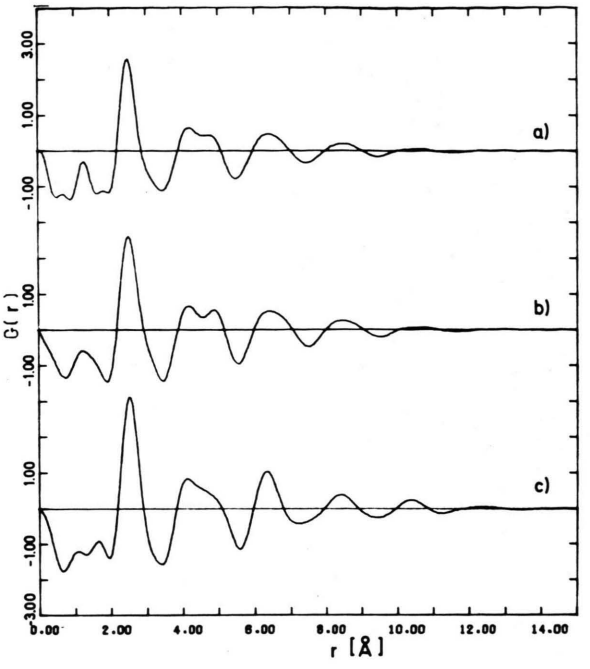

Fig. 6. Amorphous $Fe_{80}B_{20}$: Electron diffraction (50 kV). Pair correlation function $G(r)$: a) run 1; b) run 2; c) run 3.

a priori to be expected with a specimen consisting of a single element only, are discussed in detail.

The pair correlation function $G(r)$ is calculated from the structure factor as Fourier transform according to (4, 6). The coordination numbers are obtained from the function $A(r)$.

Figure 6 shows the pair correlation functions $G(r)$ for $Fe_{80}B_{20}$ as obtained from the three experimental runs. The position of the first maximum of the pair correlation function $G(r)$ and the coordination numbers N_1 for the first coordination sphere are compiled in Table 1.

The pair correlation functions of Fig. 6 are in good accordance with the functions reported in [7], which were obtained by means of electron diffraction with sputtered $Fe_{80}B_{20}$-films.

Table 1. Amorphous $Fe_{80}B_{20}$. Electron diffraction (50 kV). Multiple scattering correction parameters I/I_0, height of the first maximum $G(r_1)$ and coordination number N_1.

Material	Radiation	Thickness [Å]	I/I_0	$G(r_1)$ [Å^{-2}]	N_1	Ref.
$Fe_{80}B_{20}$	e^-	<500	0.7	2.57	12	present paper
	e^-	<500	0.38	2.61	13.4	
	e^-	<500	0.16	3.12	13	
	X	~ 300000	—	7.70	14.7	[1]

	Fe-Fe	B-B	Fe-B
e^-	0.77	0.007	0.15
X	0.79	0.002	0.008

Table 2. Weighting factors (for $Q=0$) of the partial distribution functions for $Fe_{80}B_{20}$.

In the following the specific differences between X-ray- and electron diffraction experiments shall be considered. The weighting factors in (1) are a measure for the strength with which the diffraction of the different radiations is influenced by the structure of a binary alloy. These factors are compiled for $Fe_{80}B_{20}$ in Table 2.

According to Table 2 the intensity obtained with electrons as well as with X-rays is mainly determined by the Fe-Fe-correlations. The weighting factor for Fe-B amounts to 20% of that for Fe-Fe in the case of electron diffraction. Indeed the first maximum in the pair correlation function of Fig. 6 is distinctly broader than in the case of X-ray diffraction. This broadening might be caused by the superposition of the peaks of G_{FeFe} and G_{FeB} [1]. The stronger influence of the Fe-B-pairs in the electron diffraction experiment leads furthermore to a flattening of the minimum between the two partial maxima of the second peak of $G(r)$. The differences in the three pictures of Fig. 6 may indicate some inhomogeneities of the various specimens.

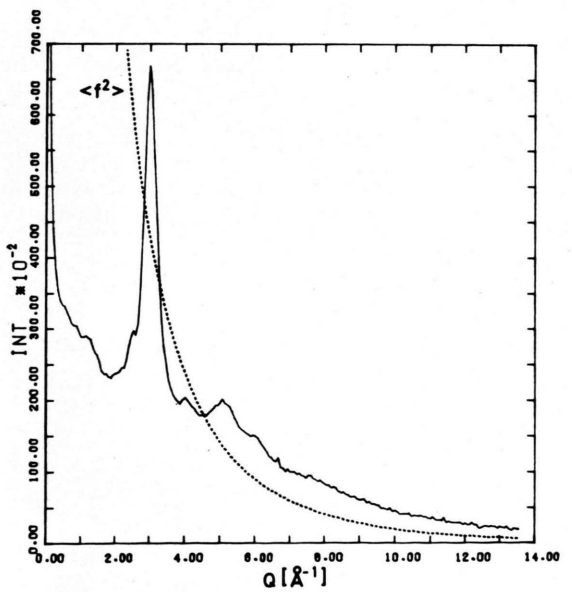

Fig. 7. Amorphous $Mn_{73}Si_{27}$: Electron diffraction (50 kV). Intensity versus Q.

ii) *Amorphous* $Mn_{73}Si_{27}$

Amorphous $Mn_{73}Si_{27}$ is very difficult to produce since the specimens obtained contain spurious crystalline regions. Electron diffraction allows, however, to analyze only the amorphous regions. We found these specimens to be very unstable; during six months they transformed rather completely into the crystalline state.

Figure 7 shows the intensity curve as obtained without correction for multiple scattering.

Figures 8 and 9 show the structure factor and the $G(r)$-curve, respectively. The coordination number N_1 and $G(r_1)$ are compiled in Table 3 together with the corresponding X-ray data.

For the comparison of the different radiations the weighting factors in (1) must be regarded, which are compiled in Table 4.

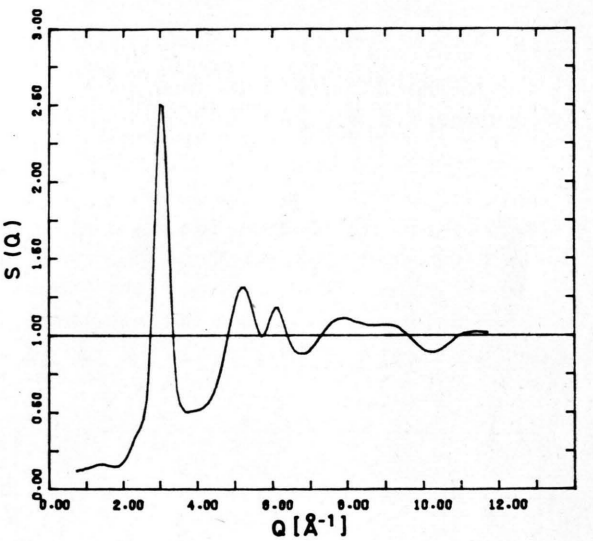

Fig. 8. Amorphous $Mn_{73}Si_{27}$: Electron diffraction (50 kV). Structure factor ($I/I_0=0.15$).

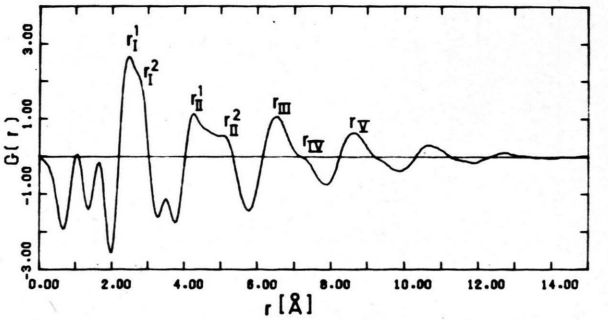

Fig. 9. Amorphous $Mn_{73}Si_{27}$: Electron diffraction (50 kV). Pair correlation function $G(r)$.

Table 3. Amorphous $Mn_{73}Si_{27}$. $G(r_1)$ and N_1 from electron diffraction- and X-ray-diffraction results.

Substance	Radiation	Thickness [Å]	I/I_0	$G(r_1)$ [Å^{-2}]	N_1	Ref.
$Mn_{73}Si_{27}$	e^-	<500	0.15	2.66	11	present paper
	X	~ 100000	—	6.6	13.5	[2]

Table 4. Amorphous $Mn_{73}Si_{27}$: Weighting factors of the partial pair distribution functions.

	Mn-Mn	Si-Si	Mn-Si
e^-	0.60	0.05	0.34
X	0.65	0.03	0.27
n	0.49	0.09	−0.42

The weighting factors for the electron- and X-ray-experiment are rather similar. Figure 10 shows the $G(r)$-curves obtained in [2] using X-rays and neutrons.

Phenomenological Model for the Nearest Neighbourhood in $Mn_{73}Si_{27}$

In [8, 9] a simple tetrahedral model is described which contains the normalized distances given in Table 5. In this table also the distances normalized to the distance of the first X-ray maximum in Fig. 10 are presented for the X-ray-, the electron- and the neutron case together with the designation of the maxima which corresponds to that in Figs. 9

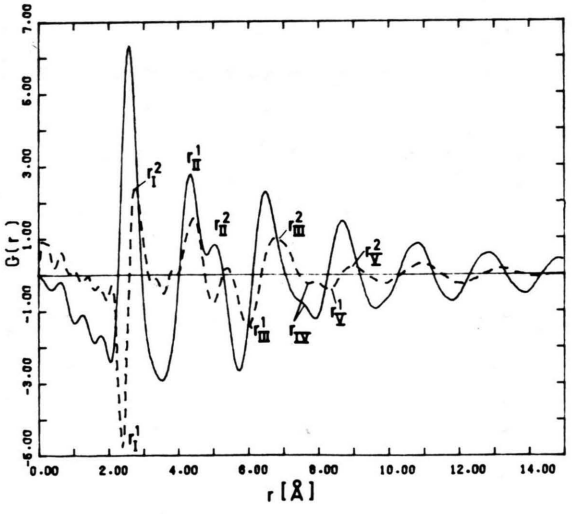

Fig. 10. Amorphous $Mn_{74}Si_{23}P_3$: Pair correlation functions, $G(r)$ according to [2]: ——— X-ray (G_{NN}); ----- neutrons (G_{CC}).

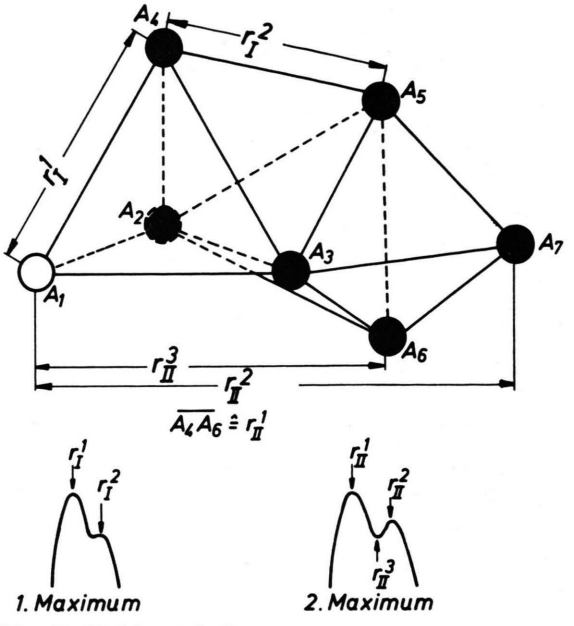

Fig. 11. Multi tetrahedra.

and 10. We state a very good coincidence of the experimental and the calculated normalized distances. In Fig. 11 an arrangement of four tetrahedra is shown. Using this figure we will discuss the differences between the X-ray curve from Fig. 10 and the electron-curve from Figure 9:

The position ($r_I^2 = 2.7$ Å) of the shoulder of the first maximum yields the radius of the Mn-atom (1.35 Å). The correspondence between the shoulder and the nearest Mn-Mn-distance is given by the result of the neutron diffraction experiment (Fig. 10, dashed curve) which corresponds to $G_{CC}(r)$. In this

Table 5. Normalized distances $r/r_I^X = r/2.59$ according to the model from Ref. [8, 9], the X-ray and neutron-experiment (Fig. 10) as well as the electron experiment (Figure 9).

	Model	X	n	e^-
r_I^1	1.00	1.00	0.90	0.94
r_I^2			1.06	1.06
r_{II}^1	1.65	1.66	1.69	1.62
r_{II}^2	1.99	1.94	1.90	1.96
r_{III}^1	2.49	2.49	2.29	2.50
r_{III}^2			2.61	
r_{IV}	2.97	2.90	2.97	2.82
r_V^1	3.38	3.33	3.21	3.30
r_V^2			3.45	

curve minima represent distances between unequal pairs and maxima represent distances between equal pairs. In the same way the main peak of the first maximum (2.45 Å) is ascribed to a Mn-Si-distance which thus yields a radius of a Si-atom (1.1 Å). The radius of the Mn-atom corresponds to the atomic radius given in the literature, whereas the radius of the Si-atom corresponds to the covalent radius. This result is in agreement to the radii given in [1] for $Fe_{80}B_{20}$ and points on strong binding between Si and Mn.

Concerning the atomic arrangement in Fig. 11 it should be mentioned that for ease in the calculation only one atom, namely A1 was chosen to be either a Si- or a Mn-atom. In reality also the one or other of the Mn-atoms A2 to A7 will be replaced by a Si-atom. In Table 6 all calculated Mn-Si- and Mn-Mn-distances around the partial maxima r_{II}^1, r_{II}^2, and r_{II}^3 are given. The normalization to $r_I = 2.59$ Å was done as in Table 5.

The comparison between the normalized distances from Table 6 with the experimental ones from Table 5 yields the following: The partial maximum r_{II}^1 lies according to Table 5 at 1.66 for the X-ray- and at 1.62 for the electron-diffraction experiment. This means that the maximum obtained with X-rays lies closer to the Mn-Mn-distances (1.70; 1.75) of Table 6 than the maximum obtained with electrons. This fact is to be expected according to the weighting factors of Table 4. However, it yields no information concerning the frequency of occurrence of the corresponding distances within the specimen. This question can be answered using the results of the neutron diffraction experiment for which according to Table 4 the totals of the weighting factors for Mn-Mn and M-Si are equal. The r_{II}^1-partial maximum in Fig. 10 measured with neutrons is positive and this means that indeed the Mn-Mn-distances at r_{II}^1 dominate within the amorphous $Mn_{73}Si_{27}$-specimen.

The partial maximum r_{II}^2 lies according to Table 5 at 1.94 for the X-ray- and at 1.96 for the electron-diffraction experiment. This means that both values are rather equal to the Mn-Si-distance of 1.99 in Table 6. Furthermore, this coincides with the fact that the neutron diffraction experiment shows at 1.90 a negative maximum which is caused by Mn-Si distances.

Attention should be drawn to the schematic presentation in the lower part of Fig. 11, in which the distances of the model are attributed to the partial maxima as obtained with the $G(R)$-curves.

	Mn-Si	Mn-Mn
r_{II}^1	1.58	1.70
r_{II}^3	1.64	1.75
r_{II}^2	1.99	2.08

Table 6. Normalized Mn-Si- and Mn-Mn-distances according to Figure 11.

Determination of the Three Partial Structure Factors by a "Three Beam Experiment"

In the following some considerations will be given concerning the possibility of the determination of the three partial structure factors S_{NN}, S_{CC}, and S_{NC} by a "three beam experiment" i.e. by combining the result of an X-ray, a neutron- and an electron diffraction experiment. The starting point is given by a system of the three linear equations (compare (8)):

$$\begin{aligned} S(Q)|_n &= w_{11} S_{NN}(Q) + w_{12} S_{CC}(Q) \\ &\quad + w_{13} S_{NC}(Q), \\ S(Q)|_x &= w_{21}(Q) S_{NN}(Q) + w_{22}(Q) S_{CC}(Q) \\ &\quad + w_{23}(Q) S_{NC}(Q), \\ S(Q)|_{e^-} &= w_{31}(Q) S_{NN}(Q) + w_{32}(Q) S_{CC}(Q) \\ &\quad + w_{33}(Q) S_{NC}(Q). \end{aligned} \tag{8}$$

The weighting factors w_{ij} for the X-ray- and the electron-diffraction experiment depend on Q as does the normalized determinant

$$[\mathrm{DET}] = \left| w_{ij}(Q) / (\Sigma_j w_{ij}^2(Q))^{1/2} \right|. \tag{9}$$

The magnitude of [DET] ($\leqq 1$) is a measure for the solubility of the system of three equations. Especially for the $Mn_{73}Si_{27}$-alloy it amounts to 0.117 for the Bhatia-Thornton-structure factors for $Q = 0$ and looks very convenient if we take into consideration the corresponding values for $Fe_{80}B_{20}$ (Ref. [1]) or $Ni_{80}B_{20}$ (Ref. [10]) of 0.06 or 0.3. These figures are valid if one performs on $Fe_{80}B_{20}$ two neutron- and one X-ray experiment and on $Ni_{80}B_{20}$ three neutron experiments.

In Fig. 12 the normalized determinant for the calculation of the Bhatia-Thornton partial structure factors for amorphous $Mn_{73}Si_{27}$ is presented versus Q for the three beam experiment. The drastical decrease of [DET] is obvious and we recognize the normalized determinant to become zero

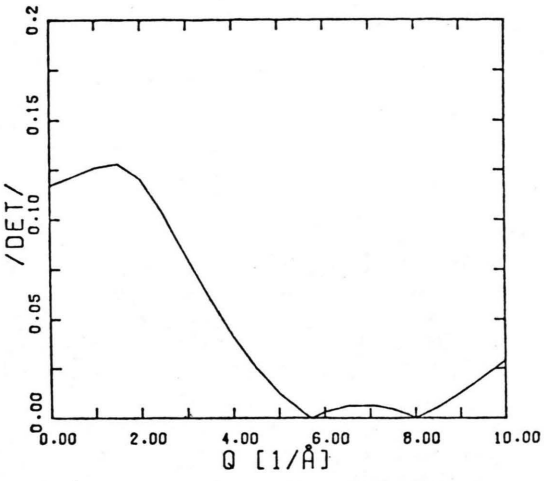

Fig. 12. Amorphous $Mn_{73}Si_{27}$: Normalized determinant for the calculation of BT-partial structure factors.

for $Q \cong 5.7$ Å^{-1}, i.e. just in the Q-region between the second and third maximum. Thus a solution of the system of three linear equations becomes impossible especially if we regard the fact that nowadays also with the very best instrumental technique available the relative experimental errors during the determination of total structure factors with amorphous specimens amount to $\pm 3\%$ for X-rays as well as neutrons and to $\pm 10\%$ for electrons. The run in Fig. 12 is the result of the fact, that the fundamental scattering process for an electron and an X-ray quantum is rather similar. The very small values for /DET/ show that a straightforward calculation of the three partial structure factors is not possible from total structure factors measured by three different radiations. This becomes evident also by the following three equations which show for $Q = 5.72$ Å^{-1} the calculation of the three partial structure factors from the three total functions:

$$\begin{aligned} S_{NN}(5.72\text{ Å}^{-1}) &= 0.07 \cdot S(Q)_n + 5895.69 \cdot S(Q)_x \\ &\quad - 5894.77 \cdot S(Q)_{e^-}, \\ S_{CC}(5.72\text{ Å}^{-1}) &= 1.55 \cdot S(Q)_n + 12902.94 \cdot S(Q)_x \\ &\quad - 12903.50 \cdot S(Q)_{e^-}, \\ S_{NC}(5.72\text{ Å}^{-1}) &= 0.15 \cdot S(Q)_n - 6446.88 \cdot S(Q)_x \\ &\quad + 6447.04 \cdot S(Q)_{e^-}. \end{aligned} \tag{10}$$

The weighting factors lead to very large uncertainties also if the experimental errors could be appreciably reduced, which at the moment seems by no means possible.

Acknowledgements

Thanks are due to the Deutsche Forschungsgemeinschaft, Bad Godesberg, for financial support of this work.

[1] E. Nold, P. Lamparter, H. Olbrich, G. Rainer-Harbach, and S. Steeb, Z. Naturforsch. **36a**, 1032 (1981).
[2] G. Rainer-Harbach, P. Lamparter, F. Paasche, and S. Steeb, Proceedings of the Fourth Int. Conference on Rapidly Quenched Metals (RQ4), Sendai, Japan, 1982, p. 315.
[3] F. Paasche, H. Olbrich, U. Schestag, P. Lamparter, and S. Steeb, Z. Naturforsch. **37a**, 1139 (1982).
[4] C. N. J. Wagner and H. Ruppersberg, Atomic Energy Review, 1981.
[5] W. Sperl, Diplomarbeit, Stuttgart 1979.
[6] J. Krogh-Moe, Acta Cryst **9**, 951 (1956).
[7] J. F. Graczyk, IEF Transactions of Magnetics **16**, 1138 (1980).
[8] P. K. Leung and J. G. Wright, Phil. Mag. **30**, 995 (1974).
[9] S. Takeuchi and S. Kobayashi, Phys. stat. sol. **65**, 315 (1981).
[10] P. Lamparter, W. Sperl, E. Nold, G. Rainer-Harbach, and S. Steeb. proceedings of the Fourth Int. Conference on Rapidly Quenched Metals (RQ4), Sendai, Japan, 1982, p. 343.